

Flame-Retardant Cellulosic Fiber Nanocomposite Based on Aluminum Tetraborate and Aluminum Tungstate

Shohreh Fakouri Nav and Hadi Fallah Moafi*

Abstract- Nanoaluminum tetraborate ($\text{Al}_2(\text{B}_4\text{O}_7)_3$) and nanoaluminum tungstate ($\text{Al}_2(\text{WO}_3)_3$) were prepared by in situ precipitation method on the surface of cellulosic fibers to achieve flame retardant nanocomposite fibers. The prepared nanocomposite fibers were characterized by several techniques such as XRD, SEM, TEM, EDS, and FTIR. $\text{Al}_2(\text{B}_4\text{O}_7)_3$ and $\text{Al}_2(\text{WO}_3)_3$ with less than 100 nm in size were dispersed throughout on the surface of the fibers without the formation of large aggregates which showed effective flame retardancy properties. It was found that loading 2.60% $\text{Al}_2(\text{B}_4\text{O}_7)_3$ and 4.95% $\text{Al}_2(\text{WO}_3)_3$ onto the cellulosic fibers improved greatly the flame retardancy behavior of nanocomposite fibers which was approved by vertical flame test and limiting oxygen index (LOI) values. The thermal stability and amount of heat release of untreated and flame retardant fibers were evaluated by thermogravimetric (TGA) and differential scanning calorimetry (DSC) analyses. The results showed that the flame retardancy mechanism of the obtained flame retardant nanocomposite fibers probably is a condensed-phase phenomenon due to the formation of a protective char layer that acts as a mass transport barrier and a thermal insulator.

Keywords: cellulosic fiber, $\text{Al}_2(\text{B}_4\text{O}_7)_3$, $\text{Al}_2(\text{WO}_3)_3$, nanocomposite, flame-retardancy

I. INTRODUCTION

The development of polymer nanocomposites using nanomaterials is one of the most important applications of nanotechnology. Polymeric materials have a variety of applications because of their exclusive properties. Polymeric materials are widely used in everyday life and so flame retardant material is often incorporated into them to diminish their flammability. The preparation of polymer nanocomposites has developed an effective solution for improving the fire retardancy of polymers using an additive

S. Fakouri Nav and H. Fallah Moafi
Department of Chemistry, Faculty of Science, University of Guilan,
Rasht, Iran.

Correspondence should be addressed to H.Fallah Moafi
e-mail: fallah.m@guilan.ac.ir

approach [1-3]. Nanomaterials with different shapes and sizes have been widely used to improve polymer composites [4]. The utilization of polymer nanocomposites with well-dispersed nanoscale particles has effectively achieved improvements in fire resistance and thermal stability of the nanocomposites [1,5,6].

Cotton fiber is the most widely used natural polymer in the field of polymer nanocomposites. Cotton fiber is one of the outstanding natural fibers utilized in the textile industry. However, cotton is flammable and has limiting oxygen index (LOI) of about 18.4%. To overcome the thermal instability and reduce the flammability of cotton, surface treatments of the fiber with durable and non-durable flame retardants are performed. The common flame retardants used for cotton fabric are mostly phosphorus- and halogen-containing flame retardant agents. The use of halogen-based flame retardants for cotton fiber is one of the most effective ways of reducing the fire hazard. However, it was recognized that the halogen-based flame retardants are not environmentally friendly, because they produce toxic and corrosive gases during thermal degradation [7,8]. In recent years, halogen-free compounds have gained much attention as flame retardant [7-9]. Some compounds, containing aluminum, silicon, magnesium, phosphorus, boron, nitrogen, and other miscellaneous elements as flame retardant in the polymer materials, have been used in replacement of halogen-based flame retardants [7-12].

Mineral filler retardants, such as metal hydroxides and metal carbonates filler retardants, have been broadly used in different polymers as halogen-free flame retardants. These flame retardant materials have an endothermic cooling mechanism and show a unique vapor/condensed phase behavior upon exposure to heat [5]. Further, the decomposition products of mineral filler flame retardants are non-flammable and their solid residues dilute the total amount of polymer fuel during the thermal decomposition. Inorganic flame retardants such as various metal oxides, metal complexes, borates, stannates, and silicates cover a wide range of mineral flame retardants that can act in both vapor and condensed phases. The main advantage of using

these flame retardants is that they are well-documented as nontoxic flame-retardant and smoke suppressant materials for a wide range of polymers and because of their mineral structure, they have little impact on the environment [5]. As mentioned above, fire retardant polymer nanocomposites have attracted considerable interest during the past few years. Polymer nanocomposites are condensed-phase flame retardants that slow the mass loss rate of the polymer through the formation of nanoparticles playing the role of thermal insulator and fire protection barrier. Scientific research has shown that the presence of nanodispersed materials, such as MnO_2 nanosheets, montmorillonite (MMT) clay, titania, silica, molybdenum disulfide, layered double hydroxides, carbon nanotubes, and nanozinc carbonate in polymeric matrices produces a substantial improvement in fire retardancy performance [13,14-20]. A large number of researches have been done on enhancing the flame retardant behavior of cotton nanocomposite using nanomaterials [21-24]. For example, Yuyang Liu *et al.* [22] fabricated the carbon nanotubes (CNTs) on the surface of cotton fibers using a simple coating method and Li *et al.* [24] reported the flame retardancy of polyelectrolyte/clay thin film assemblies on cotton fabric via layer-by-layer (LbL) assembly. The proposed mechanism for this flame-retardant behavior is an aggregation of nanoparticles on the surface of nanocomposites that forms a continuous protective solid layer on the burning surface. On the other hand, extended island structures composed of nanoparticles and carbonaceous char during burning limit the heat transfer [21,25]. However, the formation of the protective char layer as thermal insulator is clearly important in the flammability reduction by these materials. The objective of this work is to explore the flame retardancy ability of cellulose fiber treated with nanoaluminum tetraborate and nanoaluminum tungstate, prepared via *in situ* precipitation method. The treatment procedure generated an inorganic protective layer onto the cellulosic fiber to impart flame-retardant behavior.

II. EXPERIMENTAL

A. Materials

The cotton fabric with fibers of about 10-15 μm in diameter was used for the entire process. All chemicals used in this work were purchased from Merck (Germany) and used without further purification. Water used in our experiments was triply distilled.

B. Preparation of Flame-Retardant Nanocomposite Fibers

All cellulosic fabrics were a plain construction, yarns 21/10 mm, weighing 164 g.m⁻², unfinished 100% cotton, laundered, and dried. They were 22 by 8 cm strips cut along

the warp direction and pre-washed in hot distilled water for removal of impurities such as fat, wax, etc. The specimens were dried at 110 °C for 30 min in an oven, cooled in a desiccator and weighed with an analytical balance. *in situ* precipitation method was used for coating of flame retardant onto the cellulosic fabric. For the preparation of flame-retardant nanocomposite fiber, the cotton fabrics were first dipped separately into the suitable concentrations of sodium tetraborate decahydrate and sodium tungstate dihydrate solution for half an hour at 25 °C and then an aqueous solution of aluminum sulfate was added into the mixture dropwise under constant stirring for half an hour. Subsequently, white precipitates were formed onto the fabric. Afterward, the treated fabrics were squeeze-rolled, washed and dried horizontally in an oven at 110 °C for 30 min to ensure that the $\text{Al}_2(\text{B}_4\text{O}_7)_3$ and $\text{Al}_2(\text{WO}_4)_3$ nanoparticles were adhered to the surface of fibers. They were then cooled in a desiccator and re-weighed with an analytical balance so that the suitable add-on presented onto the samples was obtained. Subsequently, the treated samples were placed overnight in an average of relative humidity ranged between 65 and 67% and an average temperature ranged between 20 and 22 °C before the performance of the vertical flame test. Nanoparticles of $\text{Al}_2(\text{B}_4\text{O}_7)_3$ and $\text{Al}_2(\text{WO}_4)_3$ were synthesized during the *in situ* precipitation reaction. After that, the coated samples were separated from the reaction mixture, the white precipitate was filtered and washed and then dried at 110 °C. As a result, nanoparticles of $\text{Al}_2(\text{B}_4\text{O}_7)_3$ and $\text{Al}_2(\text{WO}_4)_3$ were obtained.

C. Flammability Test and Limiting Oxygen Index (LOI)

Flammability of the flame retardant fabric was evaluated with a vertical flame test to study the flame retardancy performance of nanocomposite fabric. A vertical flammability test method similar to the procedure described in DOC FF3-77 (U.S. Department of Commerce Standard) was used. The full description of flammability test has been demonstrated in the previous investigations [26-29].

Limiting oxygen index (LOI) was utilized to evaluate the relative flammability behavior of flame retardant nanocomposite fabric. Limiting oxygen index (LOI) values of untreated and coated fabrics were assessed according to ASTM D2863 standard method. In this order, 7 specimens of each sample were selected in 5 cm×15 cm and a mixture of oxygen and nitrogen was passed up through a cylinder containing the samples supported vertically. The minimum amount of oxygen required to support complete combustion of the fabric samples was determined and reported as the LOI value.

D. Characterization Techniques

X-ray diffraction pattern of samples was recorded using a Philips PW1820 X-ray diffractometer with Copper-K α radiation operated at 40 kV-30 mA within a range of 2 θ of 10-70° with a step size of 0.02° at room temperature. Sample morphology was investigated by a scanning electron microscope (SEM, KYKY EM-3200, 25 kV) equipped with an EDS attachment for compositional analysis. The exact particle size of the Al₂(B₄O₇)₃ and Al₂(WO₄)₃ nanoparticles were obtained by transmission electron microscopy (TEM) using a Philips CM10 instrument with an accelerating voltage of 100 kV. Infrared spectra were obtained on a Vertex70, Bruker spectrometer. To investigate the thermal behavior of samples, DSC, and TGA analyses were performed under air atmosphere at a heating rate of 10 °C·min⁻¹ using a thermogravimetric analyzer (TGA V5.1A DuPont 2000). LOI values were determined by means of an oxygen indexer (F30 Toyoseiki).

III. RESULTS AND DISCUSSION

A. Morphological and Compositional Analysis

The surface morphology and chemical composition of the untreated and flame retarded samples were determined by SEM equipped with an EDS analyzer. Fig. 1 shows SEM micrographs of untreated, flame retardant fibers, Al₂(B₄O₇)₃

and Al₂(WO₄)₃ nanoparticles. Fig. 1a is the SEM image of untreated cellulosic fiber. Fig. 1a shows that the surface of the pristine fiber is clean and grooves on the surface of the fibers are displayed. In contrast, the SEM micrograph of the treated cellulosic fibers shows that Al₂(B₄O₇)₃ and Al₂(WO₄)₃ nanoparticles are deposited on the surface of fibers. On the other hand, Figs. 1b and 1c show that treated fibers are covered by dispersed nanoparticles that are unevenly distributed over the surface of fibers. Some part of samples consisted of agglomerated particles with an approximately spherical shape and dimensions less than 100 nm (Figs. 1b and 1c). Fig. 1d is a SEM micrograph of Al₂(B₄O₇)₃ nanoparticles deposited on the fiber. The most of the nanoparticles have an approximately spherical shape with particle size ranging about 50 nm to 70 nm (Fig. 1d). Fig. 1e shows that surface morphology of Al₂(WO₄)₃ onto the fiber is similar to that of the Al₂(B₄O₇)₃ nanoparticles and nanoparticles were constructed of agglomerates of fine particles ranging from 50 nm to 70 nm (Fig. 1e).

To investigate the exact particle size of Al₂(B₄O₇)₃ and Al₂(WO₄)₃ nanoparticles forming on the fibers surface, the size of the particles was recorded by TEM, as shown in Fig. 2. TEM images show that the deposited nanoparticles consist of uniform spherical particles of average diameter of 20–60 nm. It is noticeable that the spherical Al₂(B₄O₇)₃ and

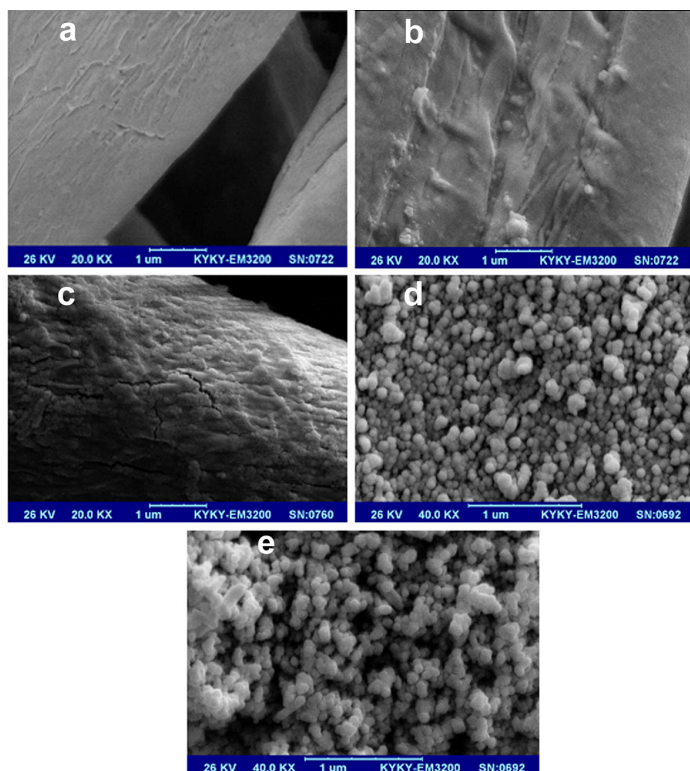


Fig. 1. SEM images of: (a) pure cellulosic fiber, (b) Al₂(B₄O₇)₃-coated fiber, (c) Al₂(WO₄)₃-coated fiber, (d) Al₂(B₄O₇)₃ nanoparticles, and (e) Al₂(WO₄)₃ nanoparticles.

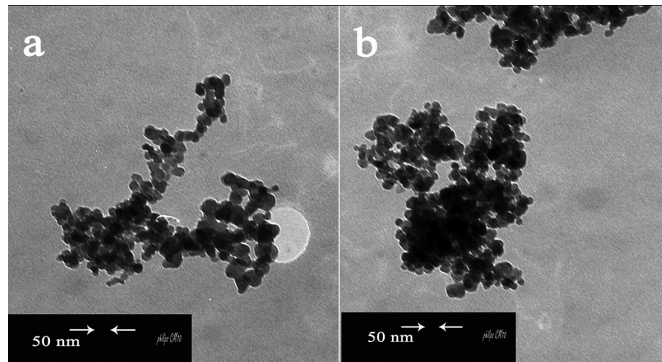


Fig. 2. TEM images of: (a) Al₂(B₄O₇)₃ and (b) Al₂(WO₄)₃ nanoparticles forming on the surface of the fibers.

Al₂(WO₄)₃ nanoparticles are distributed homogeneously on the surface of the fibers.

To check the chemical composition of the flame retardant nanocomposite fibers, EDS analysis was performed. Fig. 3 shows the EDS analysis of Al₂(B₄O₇)₃ and Al₂(WO₄)₃ coated fibers. The existence of the elements of the synthesized flame retardants can be clearly observed in the spectra. It was found that the achieved flame retardant nanocomposite fibers are consisted of C, O, Al, B, W, and no other peak is observed, which demonstrated the high purity of the flame retardant nanocomposite fibers.

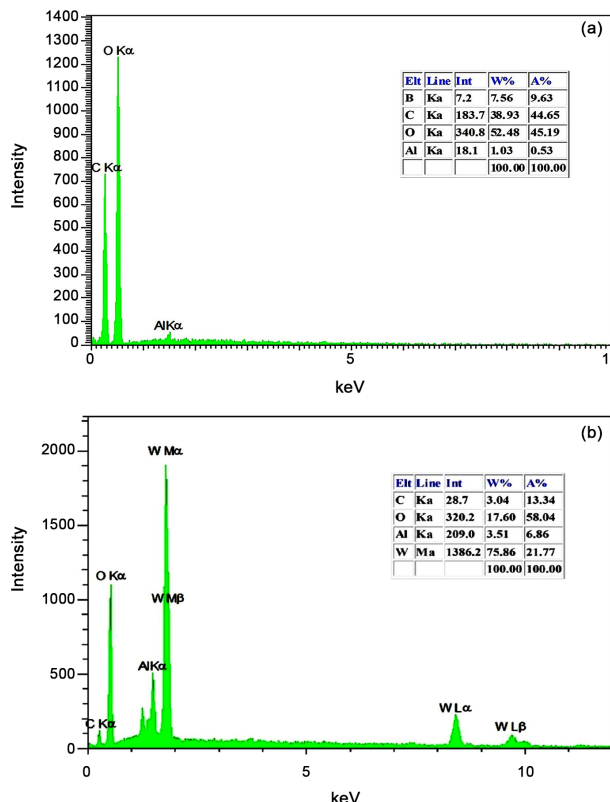


Fig. 3. EDS analysis of: (a) Al₂(B₄O₇)₃-coated fiber and (b) Al₂(WO₄)₃-coated fiber.

B. FTIR Study

Chemical structure of the untreated and flame retardant fibers was studied by FTIR spectroscopy. Fig. 4 shows the FTIR spectra of the untreated, treated cellulosic fibers, Al₂(B₄O₇)₃ and Al₂(WO₄)₃ nanoparticles measured by transmission mode. FTIR spectra of untreated fiber show the characteristic peaks of cellulose which is the main component of cotton fiber. It was observed a broad peak centered at 3416 cm⁻¹ corresponding to O–H stretching. Also, a broad peak at 3000–2800 cm⁻¹ region for C–H stretching was observed. The peak around 1639 cm⁻¹ is due to the adsorbed water molecules. Other peaks of untreated

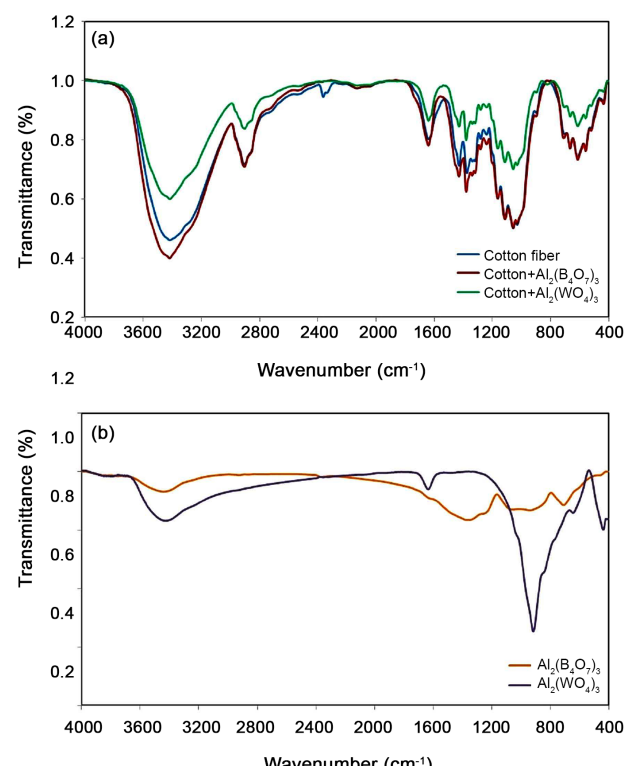


Fig. 4. FTIR spectra of: (a) pure cellulosic fiber and flame retardant coated fiber and (b) Al₂(B₄O₇)₃ and Al₂(WO₄)₃ nanoparticles.

TABLE I
BAND ASSIGNATIONS FOR THE INFRARED SPECTRUM OF PURE CELLULOSIC FABRIC AND FLAME RETARDANT FABRIC

Peak characteristics	Pure cellulosic fabric (cm^{-1})	$\text{Al}_2(\text{B}_4\text{O}_7)_3$ -coated fabric (cm^{-1})	$\text{Al}_2(\text{WO}_4)_3$ -coated fabric (cm^{-1})
H-bonded OH stretching	3650–3100	3650–3100	3650–3100
CH stretching	3000–2800	3000–2800	3000–2800
Adsorbed H_2O	1652	1656	1654
CH wagging	1432	1438	1436
In-plane bending			
CH bending (deformation stretch)	1376	1385	1385
OH in-plane bending	1240, 1337	1240, 1340	1240, 1340
CH deformation stretch	1275	1272	1273
Asym. bridge C–O–C	1168, 1120	1170, 1120	1172, 1122
Asym. in-plane ring stretch	1058	1062	1062

fiber and flame retardant fibers are assigned in Table I, as described elsewhere [30,31]. The main functional group peaks in FTIR spectra of the flame retardant fibers are entirely unchanged and structure of cellulosic fibers was not changed extensively in the flame retardant fibers, as shown in Table I. For comparison, IR spectra of $\text{Al}_2(\text{B}_4\text{O}_7)_3$ and $\text{Al}_2(\text{WO}_4)_3$ nanoparticles are shown in Fig. 4b. It is obvious that the increasing of flame retardants decreases the peak intensity of cellulosic fiber.

C. X-ray Diffraction (XRD) Analysis

The XRD patterns of pure and flame retardant coated fibers are shown in Fig. 5. The typical XRD reflections of the pure cellulosic fiber were identified. XRD pattern of pure fiber shows two broad peaks at 13.16, 15.12, and one intense peak at 21.4°, which consist of the typical XRD pattern of cellulosic fibers [32,33]. Peaks at 13.16 and 15.12° are related to the amorphous phase of cotton fiber, while the peak at 21.4° is due to the crystalline phase. Since the amount of $\text{Al}_2(\text{B}_4\text{O}_7)_3$ and $\text{Al}_2(\text{WO}_4)_3$ nanoparticles were low on the surface of the fibers, the XRD patterns of flame retardant coated fibers did not show the reflections of $\text{Al}_2(\text{B}_4\text{O}_7)_3$ and $\text{Al}_2(\text{WO}_4)_3$ phase. Meanwhile, the nanoparticles synthesized at the temperature of 110 °C on the fibers have an amorphous nature, so that they did not show the reflections in XRD pattern.

D. Flame-Retardancy Analysis

The burning characteristics of the flame retardant nanocomposite fabric obtained from the experimental tests are summarized in Tables II and III. A vertical flame test was carefully conducted to determine the add-on values on the burning time of three seconds shown in column 4

of Tables II and III. The burning rates in cm/s were calculated and shown in column 5 of Tables II and III. In the untreated sample, burning time is lower than that of the flame-retardant coated fabric. It is observed that increasing of $\text{Al}_2(\text{B}_4\text{O}_7)_3$ and $\text{Al}_2(\text{WO}_4)_3$ leads to increase the burning time. Char length of samples was measured and reported in column 6 of Tables II and III. The results showed that the performed treatment procedure decreased the flammability of the flame-retardant coated samples. In the flame retardant-coated samples, the flame extinguished immediately, thus the char length is significantly decreased. The LOI values of the untreated and flame retardant-coated fabric are shown in column 7 of Tables II and III. From Tables II and III, it is evident that the LOI value for flame retardant coated fabrics is more than that of the untreated fabrics. The LOI value of the flame retardant-treated cellulosic fabric containing 2.60% of $\text{Al}_2(\text{B}_4\text{O}_7)_3$ and 4.95% of $\text{Al}_2(\text{WO}_4)_3$ was obtained 24.3% and 25.8%,

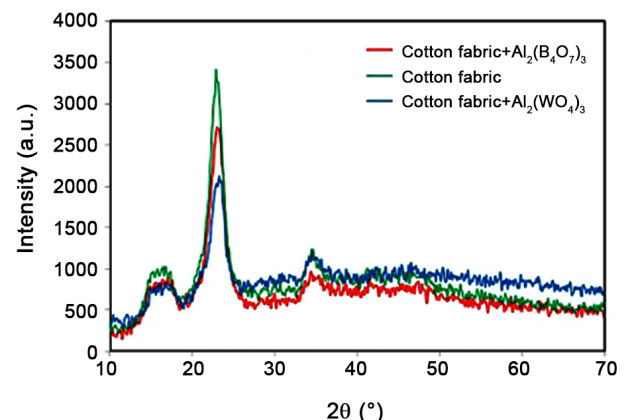


Fig. 5. XRD patterns of pure cellulosic fibers and flame retardant nanocomposite fibers.

TABLE II
THE EFFECT OF DEPOSITED ALUMINUM TETRABORATE ON THE FLAME-RETARDANCY IMPARTED TO CELLULOSIC FABRIC

Set No*	Samples	Molarity of Sodium tetraborate	Percent (add-on) of $\text{Al}_2(\text{B}_4\text{O}_7)_3$	Burning time (s)	Char length (cm)	LOI (%)	State** of the fabric
1	Untreated	-	-	24	-	18.5	CB
2	Treated	0.025	1.15	45 (as glow)	-	-	CB
3	Treated	0.050	2.60	-	1.0	24.3	FR
4	Treated	0.100	4.73	-	0.5	-	FR***
5	Treated	0.200	16.94	-	0.5	-	FR***

TABLE III
THE EFFECT OF DEPOSITED ALUMINUM TUNGSTATE ON THE FLAME-RETARDANCY IMPARTED TO CELLULOSIC FABRIC

Set No*	Samples	Molarity of sodium tungstate	Percent (add-on) of $\text{Al}_2(\text{WO}_4)_3$	Burning time (s)	Char length (cm)	LOI (%)	State** of the fabric
1	Untreated	-	-	24	-	18.5	CB
2	Treated	0.025	1.95	30	-	-	CB
3	Treated	0.050	4.95	-	2	25.8	FR
4	Treated	0.100	10.30	-	1	-	FR***
5	Treated	0.200	22.90	-	1	-	FR***

*Average of 5 tests for each set

** CB stands for completely burnt. FR means flame-retarded

*** Confirmatory tests applying excessive quantizes of flame retardant

Note 1: For flame-retardancy (FRs) samples the char length ≤ 2.0 cm

Note 2: Percent (add-on) means, the mass of addition for impregnated dry fabrics $\times 100$

respectively. The higher the LOI value shows the better the flame retardant property. It can be deduced from the column 4 that the optimal loading of nano $\text{Al}_2(\text{B}_4\text{O}_7)_3$ and nano $\text{Al}_2(\text{WO}_4)_3$ for achieving flame-retardancy is about 2.60% and 4.95%, respectively.

E. Thermal Analysis

Thermogravimetric analysis (TGA) is widely used to explore the thermal decomposition of polymers to assess their relative thermal stabilities and the pathway of combustion and pyrolysis. The TGA/DTG and DSC curves of the samples under air atmospheres are given in Figs. 6, 7, and 8. The TGA and DSC curves of untreated cellulosic fibers (Fig. 6) reveals that the pyrolysis process of cellulosic fibers includes three mass loss stages: initial, main, and char decomposition steps [34,35]. In the first stage (around 100 °C), mass loss mainly corresponds to the release of physically adsorbed water. The second stage (main pyrolysis stage) occurs in the temperature range of 250-350 °C. In this step, the mass loss is fast and significant. Most of the pyrolysis products are formed in this stage. The char pyrolysis (third stage) occurs at the temperature above

350 °C. During this process, dehydration and charring reactions are completed with the production of glucose. The carbon content in the decomposed products becomes higher and higher and charred residues are formed [34-36]. However, DSC analysis could be provided changes of temperatures of the material and the changes of the heat releasing in the pyrolysis process. DSC curve of untreated cellulosic fibers (Fig. 6) reveal that a large amount of heat is released in the second and third stages during the pyrolysis pathway (3018.13 and 5109.13 J.g⁻¹ for the second and third stage, respectively).

The TGA/DTG and DSC curves of the flame retardant coated fibers (Figs. 7 and 8) show the similar three stages as the pristine fiber and the main difference is their degradation temperatures. As expected, incorporating of $\text{Al}_2(\text{B}_4\text{O}_7)_3$ and $\text{Al}_2(\text{WO}_4)_3$ coating onto fibers decreases the initial thermo-oxidative decomposition temperature compared with that of untreated sample (Figs. 7 and 8), because of the catalytic degradation effect of $\text{Al}_2(\text{B}_4\text{O}_7)_3$ and $\text{Al}_2(\text{WO}_4)_3$, which is indicated the influence of $\text{Al}_2(\text{B}_4\text{O}_7)_3$ and $\text{Al}_2(\text{WO}_4)_3$ as a flame-retardant. Untreated fiber started rapid thermo-oxidative decomposition at 250 °C

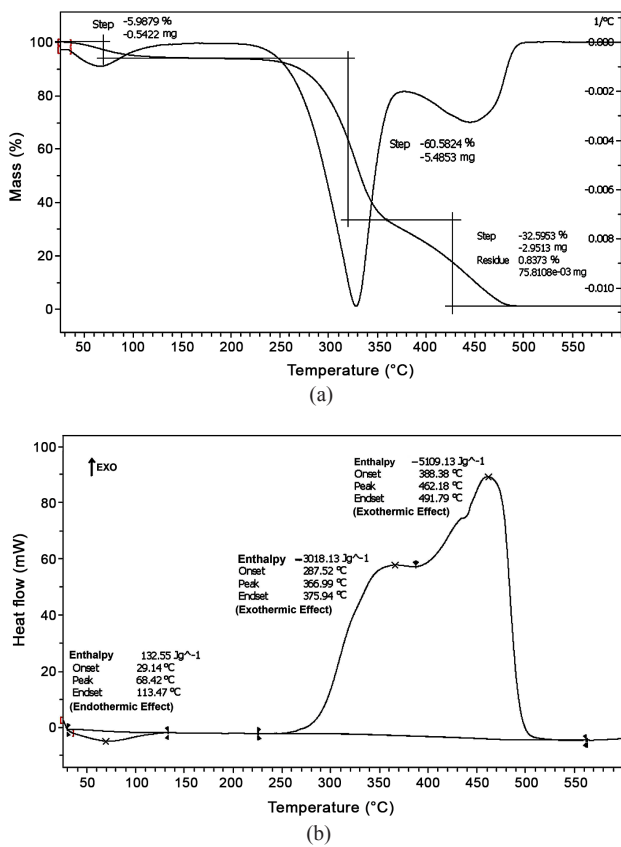
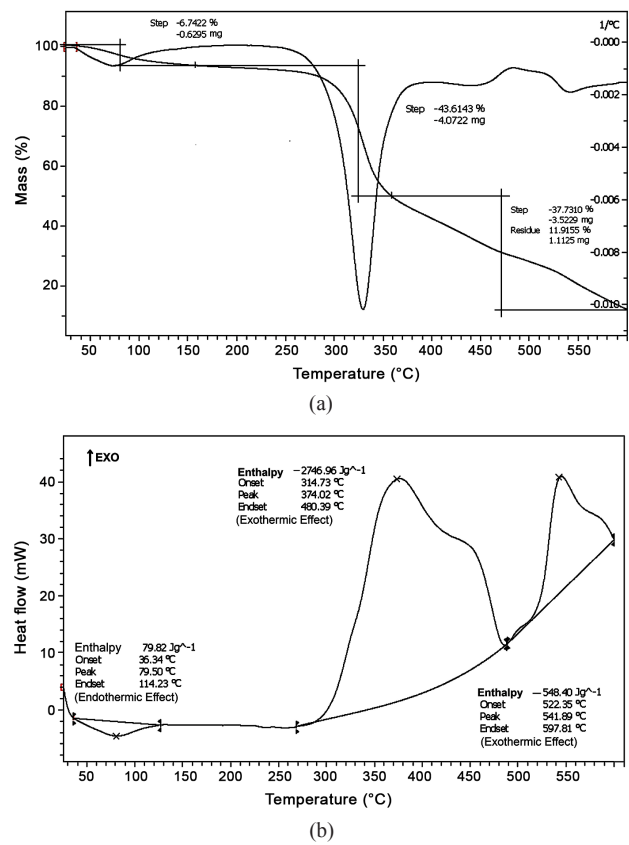
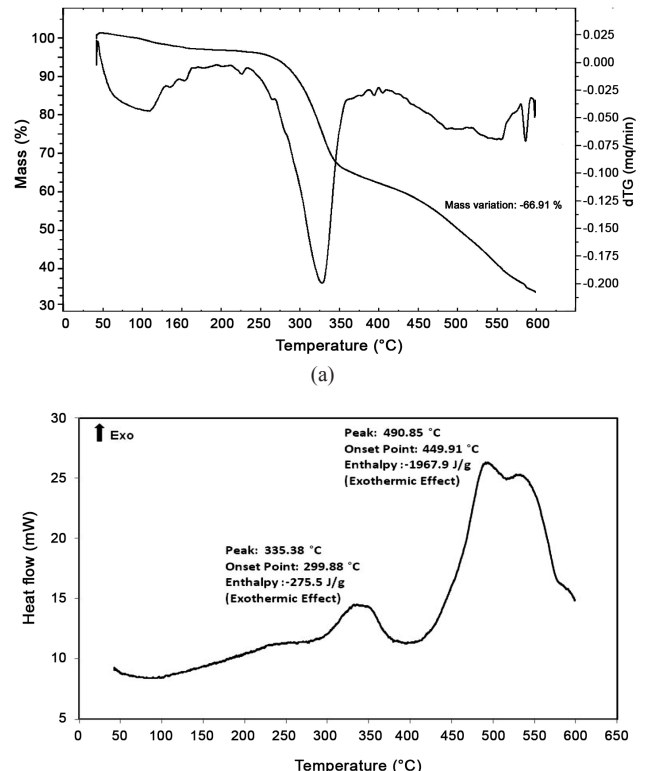


Fig. 6. TGA/DTG and DSC curves of untreated cellulosic fiber.

and lost about 99.2% of mass at 600 °C. For $\text{Al}_2(\text{B}_4\text{O}_7)_3$ -coated fiber and $\text{Al}_2(\text{WO}_4)_3$ -coated fiber, at the optimum level of loading (2.6%) of $\text{Al}_2(\text{B}_4\text{O}_7)_3$ and 4.95% $\text{Al}_2(\text{WO}_4)_3$, thermo-oxidative decomposition temperature decreased to 200 and 220 °C and 88.1 and 66.9% mass loss were observed at 600 °C, respectively. It is mentioned that for untreated fiber the major mass loss at 350 °C is 66.5%, whereas for the $\text{Al}_2(\text{B}_4\text{O}_7)_3$ and $\text{Al}_2(\text{WO}_4)_3$ treated fibers they are 50.3 and 33%, respectively. Therefore it can be deduced that by using $\text{Al}_2(\text{B}_4\text{O}_7)_3$ and $\text{Al}_2(\text{WO}_4)_3$ as flame-retardant, the formation of volatile pyrolysis products has been postponed, when the polymer is subjected to the thermo-oxidative decomposition.

It can be clearly seen from the DSC curves that the addition of $\text{Al}_2(\text{B}_4\text{O}_7)_3$ and $\text{Al}_2(\text{WO}_4)_3$ decreases the heat released during the combustion pathway (Figs. 7 and 8), implying the influence of $\text{Al}_2(\text{B}_4\text{O}_7)_3$ and $\text{Al}_2(\text{WO}_4)_3$ as efficient flame retardants. For $\text{Al}_2(\text{B}_4\text{O}_7)_3$ -treated fiber, the values of the heat released in the second and third stages of thermo-oxidative decomposition were 2746.96 and 548.40 J.g⁻¹, and for $\text{Al}_2(\text{WO}_4)_3$ -treated fiber they were 275.50 and 1967.90 J.g⁻¹. The lower pyrolysis heat observed for flame retardant coated samples can be attributed to the catalytic action of $\text{Al}_2(\text{B}_4\text{O}_7)_3$ and $\text{Al}_2(\text{WO}_4)_3$ which enables fibers to be dehydrated at a lower temperature and char

Fig. 7. TGA/DTG and DSC curves of $\text{Al}_2(\text{B}_4\text{O}_7)_3$ -treated cellulosic fiber.Fig. 8. TGA/DTG and DSC curves of $\text{Al}_2(\text{WO}_4)_3$ treated cellulosic fiber.

to be formed faster. Also, the remaining residue of flame retardant, i.e. $\text{Al}_2(\text{B}_4\text{O}_7)_3$ and $\text{Al}_2(\text{WO}_4)_3$ seems to play the role of dust or wall in heat absorption and dissipation in the combustion zone. On the other hand, the flame retardancy action of $\text{Al}_2(\text{B}_4\text{O}_7)_3$ and $\text{Al}_2(\text{WO}_4)_3$ can be attributed to the dust or wall theory [28,29]. According to this theory, “if a high enough concentration of dust is present in the air, no flame can propagate”. This phenomenon occurs by the absorption and dissipation of heat by the inert dust which reduces the temperature and prevents further burning of the polymer. Meanwhile, the flame retardancy behavior of $\text{Al}_2(\text{B}_4\text{O}_7)_3$ and $\text{Al}_2(\text{WO}_4)_3$ nanoparticles can be attributed to their ability to form a protective char layer that acts as a mass transport barrier and a thermal insulator. This heat-shielding layer decelerates the escape of volatile products generated from the degrading polymer [3]. The reduction of the mass loss rate, and the increasing in the char yield, suggested that the mechanism of flame retardancy is likely a condensed-phase phenomenon due to the formation of a thermal protection/mass loss barrier, that leading to a retardation of the flame.

IV. CONCLUSION

This study focused on synthesis of $\text{Al}_2(\text{B}_4\text{O}_7)_3$ and $\text{Al}_2(\text{WO}_4)_3$ nanoparticles using *in situ* precipitation method, with the goal of developing a flame-retardant coating system for cellulosic fabrics. The morphology, dispersion and particle size of $\text{Al}_2(\text{B}_4\text{O}_7)_3$ and $\text{Al}_2(\text{WO}_4)_3$ nanoparticles on the fabric were studied by SEM and TEM. The used $\text{Al}_2(\text{B}_4\text{O}_7)_3$ and $\text{Al}_2(\text{WO}_4)_3$ flame retardants with 20-60 nm in size was found to be well-dispersed throughout on the surface of fibers without the formation of large aggregates. The optimum loadings to impart flame-retardancy were about 2.60 and 4.95% for $\text{Al}_2(\text{B}_4\text{O}_7)_3$ and $\text{Al}_2(\text{WO}_4)_3$, respectively. Flame retardancy potential of the nanocomposite fibers was tested by the vertical flame test, limiting oxygen index and thermal analysis. TGA/DTG and DSC analyses revealed that the addition of nano $\text{Al}_2(\text{B}_4\text{O}_7)_3$ and $\text{Al}_2(\text{WO}_4)_3$ reduced the mass loss rate, thermo-oxidative decomposition temperature and heat releasing in flame retardant nanocomposite fabric. The increases in the char yield and a reduction in the mass loss rate supported by TGA analysis suggest that the flame retardancy mechanism of flame retardant nanocomposites is likely a condensed-phase phenomenon due to the formation of a thermal barrier coating which could improve the fire property of flame retardant coated fiber.

ACKNOWLEDGMENT

The authors are grateful to the University of Guilan for

financial assistance of this research project.

REFERENCES

- [1] N.F. Attia, N.S. Abd El-Aal, and M.A. Hassan, “Facile synthesis of graphene sheets decorated nanoparticles and flammability of their polymer nanocomposites”, *Polym. Degrad. Stabil.*, vol. 126, pp. 65-74, 2016.
- [2] S. Bourbigot and S. Duquesne, “Fire retardant polymers: recent developments and opportunities”, *J. Mater. Chem.*, vol. 17, no. 22, pp. 2283-2300, 2007.
- [3] A.L. Higginbotham, J.R. Lomeda, A.B. Morgan, and J.M. Tour, “Graphite oxide flame-retardant polymer nanocomposites”, *ACS Appl. Mater. Inter.*, vol. 1, no. 10, pp. 2256-2261, 2009.
- [4] N.F. Attia, J.P. Rao, and K.E. Geckeler, “Nanodiamond-polymer nanoparticle composites and their thin films”, *J. Nanopart. Res.*, vol. 16, pp. 2361, 2014.
- [5] A.B. Morgan and J.W. Gilman, “An overview of flame retardancy of polymeric materials: application, technology, and future directions”, *Fire Mater.*, vol. 37, pp. 259-279, 2013.
- [6] J.Z. Liang, J.Q. Feng, C.P. Tsui, C.Y. Tang, D.F. Liu, S.D. Zhang, and W.F. Huang, “Mechanical properties and flame-retardant of PP/MRP/Mg(OH)₂/Al(OH)₃ composites”, *Compos. B: Eng.*, vol. 71, pp. 74-81, 2015.
- [7] Z. Bin, L. Hong, and H. Jian, “Aluminum phosphate microcapsule flame retardants for flexible polyurethane foams”, *J. Phys. Chem. Solids*, vol. 115, pp. 199-207, 2018.
- [8] Z. Liyong, Z. Min, L. Jiyan, L. Xueqing, C. Jia, H. Quan, and Peng. Sha, “Flame-retardant thermoplastic polyester based on multiarm aluminum phosphinate for improving anti-dripping”, *Thermochim. Acta*, vol. 664, pp. 118-127, 2018.
- [9] L. Yunhua, W. Chifei, and X. Shuai, “Mechanical, thermal and flame retardant properties of magnesium hydroxide filled poly(vinyl chloride) composites: the effect of filler shape”, *Compos. Part A: Appl. Sci. Manuf.*, vol. 113, pp. 1-11, 2018.
- [10] Z. Shariatinia, N. Javeri, and S. Shekariz, “Flame retardant cotton fibers produced using novel synthesized halogen-free phosphoramide nanoparticles”, *Carbohyd. Polym.*, vol. 118, pp. 183-198, 2015.
- [11] W. Dong, M. Xiaowei, C. Wei, S. Lei, M. Chao, and H. Yuan, “Constructing phosphorus, nitrogen, silicon-co-contained boron nitride nanosheets to reinforce flame retardant properties of unsaturated polyester resin”, *Compos. Part A: Appl. Sci. Manuf.*, vol. 109, pp. 546-554, 2018.

- [12] Q. Shuilai, H. Yanbei, X. Weiyi, M. Chao, Z. Xia, L. Longxiang, K. Yongchun et al., "Self-assembled supermolecular aggregate supported on boron nitride nanoplatelets for flame retardant and friction application", *Chem. Eng. J.*, vol. 349, pp. 223-234, 2018.
- [13] W. Wei, P. Ying, P. Haifeng, Y. Wei, K.M. Liew, S. Lei, and H. Yuan, "Synthesis and characterization of MnO₂ nanosheets based multilayer coating and applications as a flame retardant for flexible polyurethane foam", *Compos. Sci. Technol.*, vol. 123, pp. 212-221, 2016.
- [14] Y. Pan, W. Wang, H. Pan, J. Zhan, and Y. Hu, "Fabrication of montmorillonite and titanate nanotube based coatings via layer-by-layer self-assembly method to enhance the thermal stability, flame retardancy and ultraviolet protection of polyethylene terephthalate (PET) fabric", *RSC Adv.*, vol. 6, pp. 53625-53634, 2016.
- [15] C. Xian-Wei, G. Jin-Ping, Y. Xu-Hong, and T. Ren-Cheng, "Durable flame retardant wool fabric treated by phytic acid and TiO₂ using an exhaustion-assisted pad-dry-cure process", *Thermochim. Acta*, vol. 665, pp. 28-36, 2018.
- [16] Z. Qiang-hua, G. Jiali, C. Guo-qiang, and X. Tie-ling, "Durable flame retardant finish for silk fabric using boron hybrid silica sol", *Appl. Surf. Sci.*, vol. 387, pp. 446-453, 2016.
- [17] Q. Shuilai, H. Yixin, S. Yongqian, H. Yanbei, K. Yongchun, C. Fukai, S. Haibo et al., "In situ growth of polyphosphazene particles on molybdenum disulfide nanosheets for flame retardant and friction application", *Compos. Part A: Appl. Sci. Manuf.*, vol. 114, pp. 407-417, 2018.
- [18] Z. Sheng, Y. Yongxin, W. Wenji, G. Xiaoyu, L. Hongfei, L. Jianhua, and S. Jun, "Intercalation of phosphotungstic acid into layered double hydroxides by reconstruction method and its application in intumescent flame retardant poly(lactic acid) composites", *Polym. Degrad. Stabil.*, vol. 147, pp. 142-150, 2018.
- [19] J. Xiaoying, C. Dayong, W. Qingwen, S. Jiabin, and G. Shaoyun, "Synergistic effect of flame retardants and carbon nanotubes on flame retarding and electromagnetic shielding properties of thermoplastic polyurethane", *Compos. Sci. Technol.*, vol. 163, pp. 49-55, 2018.
- [20] Y. Pan and D. Wang, "One-step hydrothermal synthesis of nano zinc carbonate and its use as a promising substitute for antimony trioxide in flame retardant flexible poly(vinyl chloride)", *RSC Adv.*, vol. 5, pp. 27837- 27843, 2015.
- [21] G. Laufer, F. Carosio, R. Martinez, G. Camino, and J.C. Grunlan, "Growth and fire resistance of colloidal silica-polyelectrolyte thin film assemblies", *J. Colloid Interf. Sci.*, vol. 356, pp. 69-77, 2011.
- [22] Y. Liu, X. Wang, K. Qi, and J.H. Xin, "Functionalization of cotton with carbon nanotubes", *J. Mater. Chem.*, vol. 18, pp. 3454-3460, 2008.
- [23] J. Alongi, J. Tata, and A. Frache, "Hydrotalcite and nanometric silica as finishing additives to enhance the thermal stability and flame retardancy of cotton", *Cellulose*, vol. 18, pp. 179-190, 2011.
- [24] Y.C. Li, J. Schulz, S. Mannen, C. Delhom, B. Condon, S. Chang, M. Zammarano et al., "Flame retardant behavior of polyelectrolyte clay thin film assemblies on cotton fabric", *ACS Nano.*, vol. 4, pp. 3325-3337, 2010.
- [25] T. Kashiwagi, F. Du, J.F. Douglas, K.I. Winey, R.H. Harris Jr, and J.R. Shields, "Nanoparticle networks reduce the flammability of polymer nanocomposites", *Nature Mater.*, vol. 4, pp. 928-933, 2005.
- [26] H.F. Moafi and S.M. Mostashari, "Flame-resistant polymeric composite fibers based on nanocoating flame retardant: thermogravimetric study and production of α -Al₂O₃ nanoparticles by flame combustion", *J. Polym. Eng.*, vol. 34, no. 9, pp. 803-812, 2014.
- [27] S.M. Mostashari and H.F. Moafi, "Thermal decomposition pathway of a cellulosic fabric impregnated by magnesium chloride hexahydrate as a flame-retardant", *J. Therm. Anal. Calorim.*, vol. 93, no. 2, pp. 589-594, 2008.
- [28] H.F. Moafi, A.F. Shojaie, and M.A. Zanjanchi, "Flame-retardancy and photocatalytic properties of cellulosic fabric coated by nano-sized titanium dioxide", *J. Therm. Anal. Calorim.*, vol. 104, no. 2, pp. 717-724, 2011.
- [29] H.F. Moafi, A.F. Shojaie, and M.A. Zanjanchi, "Synthesis and characterization of nano-sized zinc oxide coating on cellulosic fibers: photoactivity and flame-retardancy study", *Chin. J. Chem.*, vol. 29, pp. 1239-1245, 2011.
- [30] C. Chinkap, L. Myunghee, and C. Eun Kyung, "Characterization of cotton fabric scouring by FT-IR ATR spectroscopy", *Carbohyd. Polym.*, vol. 58, pp. 417-420, 2004.
- [31] R. Chen, K. Jakes, R. Chen, and K. Jakes, "Effects of pressing on the infrared spectra of single cotton fibers", *Appl. Spectrosc.*, vol. 56, pp. 646-650, 2002.
- [32] N. Longhui, W. Jie, and Yu. Jiaguo, "Preparation of a Pt/TiO₂/cotton fiber composite catalyst with low air resistance for E-cient formaldehyde oxidation at room temperature", *RSC Adv.*, vol. 7, pp. 21389- 21397,

2017.

- [33] R. Rahal, T. Pigot, D. Foix, and S. Lacombe, “Photocatalytic efficiency and self-cleaning properties under visible light of cotton fabrics coated with sensitized TiO₂”, *Appl. Catal. B: Environ.*, vol. 104, pp. 361–372, 2011.
- [34] P. Zhu, S. Sui, B. Wang, K. Sun, and G. Sun, “A study of pyrolysis and pyrolysis products of flame-retardant cotton fabrics by DSC, TGA, and PY–GC–MS”, *J. Anal. Appl. Pyrol.*, vol. 71, pp. 645–655, 2004.
- [35] G. Sabyasachi, R. Patrick, S. Viktoriya, H. Manfred, R. Stefan, and V. Frederic, “Thermal decomposition and burning behavior of cellulose treated with ethyl ester phosphoramidates: effect of alkyl substituent on nitrogen atom”, *Polym. Degrad. Stabil.*, vol. 94, pp. 1125–1134, 2009.
- [36] X. Weiyi, J. Ganxin, S. Lei, H. Shuang, L. Xiaoqi, W. Xin, and H. Yuan, “Flame retardancy and thermal degradation of cotton textiles based on UV-curable flame retardant coatings”, *Thermochim. Acta*, vol. 513, pp. 75–82, 2011.